JGP Journal of General Physiology

ARTICLE

Catecholamines are key modulators of ventricular repolarization patterns in the ball python (*Python regius*)

Bastiaan J.D. Boukens[1], William Joyce[2], Ditte Lind Kristensen[2], Ingeborg Hooijkaas[1], Aldo Jongejan[3], Tobias Wang[2], and Bjarke Jensen[1]

Ectothermic vertebrates experience daily changes in body temperature, and anecdotal observations suggest these changes affect ventricular repolarization such that the T-wave in the ECG changes polarity. Mammals, in contrast, can maintain stable body temperatures, and their ventricular repolarization is strongly modulated by changes in heart rate and by sympathetic nervous system activity. The aim of this study was to assess the role of body temperature, heart rate, and circulating catecholamines on local repolarization gradients in the ectothermic ball python (*Python regius*). We recorded body-surface electrocardiograms and performed open-chest high-resolution epicardial mapping while increasing body temperature in five pythons, in all of which there was a change in T-wave polarity. However, the vector of repolarization differed between individuals, and only a subset of leads revealed T-wave polarity change. RNA sequencing revealed regional differences related to adrenergic signaling. In one denervated and Ringer's solution–perfused heart, heating and elevated heart rates did not induce change in T-wave polarity, whereas noradrenaline did. Accordingly, electrocardiograms in eight awake pythons receiving intra-arterial infusion of the β-adrenergic receptor agonists adrenaline and isoproterenol revealed T-wave inversion in most individuals. Conversely, blocking the β-adrenergic receptors using propranolol prevented T-wave change during heating. Our findings indicate that changes in ventricular repolarization in ball pythons are caused by increased tone of the sympathetic nervous system, not by changes in temperature. Therefore, ventricular repolarization in both pythons and mammals is modulated by evolutionary conserved mechanisms involving catecholaminergic stimulation.

Introduction

The T-wave in the electrocardiogram (ECG) stems from differences in local ventricular repolarization (Noble and Cohen, 1978; Burdon-Sanderson, 1880). When repolarization differences are augmented, for example by temperature, stress, or genetic predisposition, the risk of life-threatening arrhythmias increases (Locati et al., 2019). Early experiments on ectothermic vertebrates, including reptiles, described that the T-wave morphology is related to regional differences in action potential duration (Burdon-Sanderson, 1880; Mines, 1913). The morphology of the T-wave and the duration of the QT-interval depend on heart rate (HR), which is strongly modulated by the autonomic nervous system. The autonomic regulation of HR is evolutionary conserved among vertebrates (Taylor et al., 2014), but it remains unknown whether the autonomic nervous system affects ventricular repolarization in ectothermic vertebrates. From a biomedical perspective, the evolutionary conservation of these electrophysiological processes is relevant because ectothermic organisms, such as zebrafish or *Xenopus laevis*, have become popular model organisms for studying the effect of drugs on ventricular repolarization (Milan et al., 2006; MacRae and Peterson, 2015; Vornanen, 2016; Corbin-Leftwich et al., 2018).

In the ECG of ectotherms, similar deflections can be observed as in the ECG of mammals. This includes a clear T-wave (Vaykshnorayte et al., 2011), and a P-wave and a QRS complex caused by atrial and ventricular depolarization, respectively (Fig. 1). However, QT-interval and T-wave durations are much longer in ectotherms than in mammals when measured at similar body temperature (37°C) and comparable HRs (Boukens et al., 2019). In reptiles, the T-wave is typically negative and discordant with the QRS complex (Fig. 1). Anecdotal observations on a few species of reptiles, however, show that the T-wave is transiently positive when body temperature changes (McDonald and Heath, 1971; Mullen, 1967; Valentinuzzi et al., 1969; Zaar et al., 2004). In ectotherms, the change in

[1]University of Amsterdam, Amsterdam UMC, Department of Medical Biology, Amsterdam Cardiovascular Sciences, Amsterdam, The Netherlands; [2]Department of Biology, Zoophysiology, Aarhus University, Aarhus, Denmark; [3]University of Amsterdam, Amsterdam UMC, Department of Epidemiology & Data Science, Amsterdam, The Netherlands.

Correspondence to Bastiaan J.D. Boukens: b.j.boukens@amsterdamumc.nl; Bjarke Jensen: b.jensen@amsterdamumc.nl.

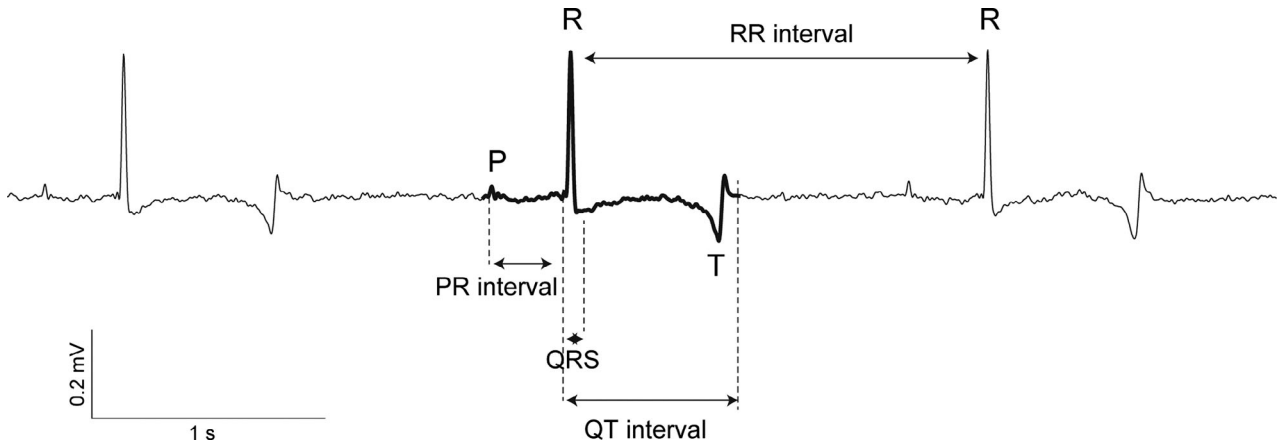

Figure 1. **Typical example of an ECG recorded from an anesthetized python.**

metabolism when body temperature changes is associated with altered autonomic tone on the heart and vasculature (Galli et al., 2004; Seebacher and Franklin, 2001). If the change in T-wave polarity at higher body temperatures is due to altered autonomic tone, it could indicate evolutionary conservation of autonomic modulation of repolarization.

Positive T-waves have been documented at high temperatures in some, but not all, individuals of multiple species of reptiles, including the boa constrictor, a species of snake (Valentinuzzi et al., 1969). Here, we investigated the role of heating, HR change, and sympathetic tone on T-wave polarity in the ball python. We selected ball pythons because they are ectothermic and tolerate high body temperatures (>35°C; Fobian et al., 2014). Moreover, because snakes lack a sternum, the heart is easily accessible for recording local electrograms. Finally, pythons are the only snakes in which functionally separated ventricles have evolved with a high-pressure left side and a low-pressure right side (Jensen et al., 2014), and in this way pythons resemble mammals more than most ectotherms. Our data indicate that catecholamines released during heating, and not temperature itself, underlie changes in T-wave morphology. Moreover, we show that genes encoding key receptors are expressed in the ventricular myocardium of pythons, indicating evolutionary conservation of aspects of the autonomic nervous system.

Materials and methods

All studies were performed in accordance with the rules and regulations for animal experiments as outlined by the national Danish animals care inspectorate (Dyreforsøgstilsynet) and were done in accordance with local animal care regulations.

ECG and local electrograms in five anesthetized pythons during heating

We used five adult ball pythons (*Python regius*) that were bought commercially from Leo Shaudy and transported to the Institute of Biology, Zoophysiology, Aarhus University, Aarhus, Denmark. Animals were maintained in 72 cm × 40 cm × 20 cm (31-liter) plastic boxes at 26°C (room temperature; relative humidity, 80%; heading pad provided for each snake, 32°C) with free access to water. Animals were fed an ad libitum diet of mice and rats. All snakes appeared healthy and were eating regularly before the study. Average body mass in the first experiment was 903 ± 193 g. Snakes were fasted at least 7 d before experiments, and none were shedding. On the day of study, the pythons were lightly anesthetized by placing them in a sealed container with gauze soaked in isoflurane (IsoFlo Vet 100%; Orion Pharma Animal Health AS). Once reflexes to pinching had subsided, the animal's trachea was intubated with 0.5-cm-diameter soft polyethylene (made from 3.5-ml pipettes; Sarstedt AG & Co.). The tubing was connected to a recycling-oxygen ventilator (Anesthesia Workstation; Hallowell EMC) and a vaporizer with isoflurane (Fluotec Mark 3 vaporizer; Simonsen & Well A/S) providing 2% isoflurane in a total volume of 200 ml of air $kg^{-1} \times min^{-1}$ delivered in 4 breaths min^{-1}. Once a surgical plane of anesthesia was achieved, the animal was placed ventral side up on a heating mat (Melissa Electric Heating Pad 631–109; Adexi A/S). The heart was then exposed by a ventrolateral incision and the pericardium opened for the placement of the multi-electrode on the heart. Fig. 2 B shows the placement of the ECG electrodes. Two electrodes were subcutaneously placed immediately cranial to the heart on the left and right side, and a third electrode was placed immediately caudal to the heart on the snake's left. ECGs were recorded using an amplifier (AD Instruments 15T), and a standard six-lead ECG was calculated as follows: I = L − R, II = F − R, III = F − L, aVR = R − (L + F)/2, aVL = L − (R + F)/2, and aVF = F − (L + R)/2. Local electrograms from the ventral surface were simultaneously recorded using a custom-made 256-lead electrode grid via a multichannel data acquisition system (24-bit dynamic range, 122.07 nV LSB, total noise 0.5 µV; BioSemi), previously described in detail (Wiegerinck et al., 2006). Temperature recordings were obtained from an electrode placed next to the heart inside the exposed body cavity and connected to a thermocouple (made in-house, Aarhus University). The thermocouple was calibrated daily using a mercury thermometer and hot and ice-cold water. A second heat mat was then placed on the snake except for the region of the heart. Once satisfactory baseline recordings could be collected at room temperature, heating commenced. Once the heating mats were

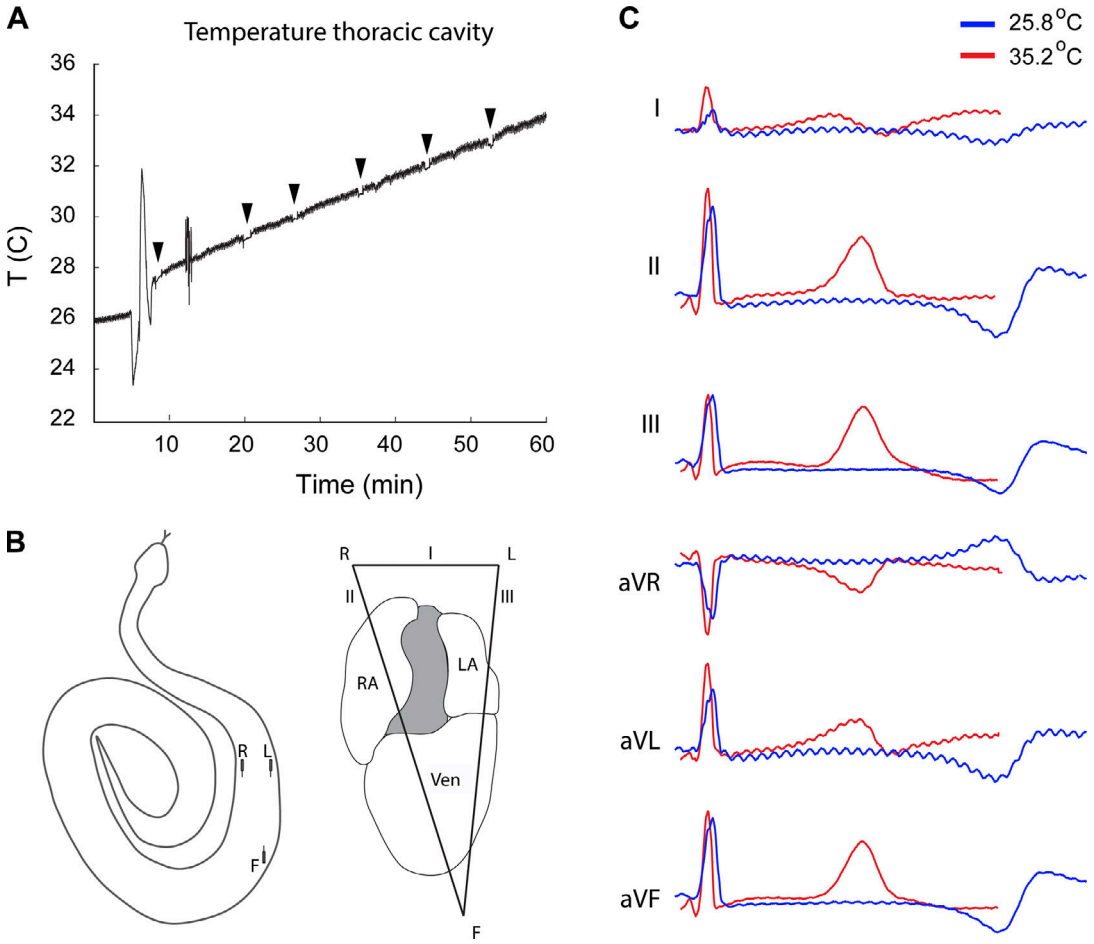

Figure 2. **Increasing body temperature induces T-wave inversion in pythons. (A)** The graph shows a representative trace of temperature measured in the thorax of a python during the heating protocol. Electrode recordings were made in brief intervals (black arrowheads) in which the heating pads were disconnected to reduce noise. **(B)** A schematic drawing (left) of a python and its heart (right) showing the location of the body surface electrodes. **(C)** A six-lead ECG recorded at 25.8°C (blue) and 35.2°C (red) of python 3. Note the change in T-wave polarity in each lead. We observed change in T-wave polarity in five snakes. F, foot electrode; L, left electrode; LA, left atrium; R, right electrode; RA, right atrium; Ven, ventricle.

connected to the power outlet, we recorded substantial noise in the electrical recordings. Consequently, the mats were unplugged at approximately every 1°C increment in body temperature, and local recordings were made (Fig. 2 A). Animal core body temperature was increased such from ∼25 to 35°C. At the completion of the study, the heart was excised, and the animals received an intra-arterial injection of pentobarbital (200 mg kg^{-1}).

RNA sequencing

After excision of the heart, transmural tissue samples from the left and right ventricular were collected (4 mm^3). The samples were briefly rinsed with sterile physiological saline (9 g $liter^{-1}$ NaCl) and blotted on tissue paper to remove most cavity fluid. Each sample was then placed in a 1.5-ml Eppendorf tube, left in liquid nitrogen for ∼10 min, and then stored at −80°C. Later the samples were sent on dry ice from Aarhus, Denmark, to Amsterdam, The Netherlands.

In Amsterdam, RNA was isolated using TruSeq (Illumina) and sequenced using Illumina Hiseq 4000 (sequence length 50, single end). Reads are subjected to quality control (FastQC; Picard Tools), trimmed using Trimmomatic v0.32 (Bolger et al., 2014), and aligned to the genome using HISAT2 (v2.0.4; Kim et al., 2015) with default settings. The genome of the Burmese python (*Python bivittatus*) and its annotation were obtained from the National Center for Biotechnology Information (genome build 5.0.2, RefSeq assembly GCF_000186305.1). Counts were obtained using HTSeq (v0.6.1; Anders et al., 2015). Statistical analyses were performed using the edgeR (Robinson et al., 2010) and limma/voom (Ritchie et al., 2015) R packages. First, all features with no counts in any of the samples were removed (leaving 18,365 from 20,064 initial features). Then, using the filtering described here, a further 2,694 were removed, leaving a final 15,671 features. Count data are transformed to log2-counts per million, normalized by applying the trimmed mean of M-values method (Robinson et al., 2010), and precision weighted using voom. Differential expression is assessed using an empirical Bayes moderated *t* test within limma's linear model framework including the precision weights estimated by voom and correcting for the python individual. Resulting P values are corrected for multiple testing using the Benjamini–Hochberg false discovery rate. The analysis was performed using R version

3.4.1. Heatmap clustering using Pheatmap: Unsupervised hierarchical clustering was performed on genes that were detected to be differentially expressed in RNA sequencing (P adjusted < 0.1) using the R package pheatmap, version 1.0.8 (http://cran.r-project.org/web/packages/pheatmap/index.html). Kyoto Encyclopedia Genes and Genomes (KEGG) pathways analysis using DAVID (Huang et al., 2009) was used to find overrepresented KEGG pathways. Benjamini–Hochberg correction was performed for multiple testing–controlled P values. Significantly enriched terms were functionally grouped and visualized.

In situ perfused heart preparation of a single python

One python (body mass, 950 g) was sacrificed (isofluorane anesthesia followed by decapitation and pithing) and an in situ perfused heart preparation was established as described (Joyce et al., 2016). Briefly, the posterior caval vein (supplying the sinus venosus and right atrium) and the pulmonary vein (supplying the left atrium) were cannulated with custom-made double-bore stainless steel cannulae, allowing simultaneous perfusion and measurement of preload pressure. All other major veins in proximity to the heart were ligated with surgical silk. Immediately cranial to the heart, the right and left aortic arches and pulmonary artery were cannulated with double-bore polyethylene catheters and connected to height-adjustable columns to set physiological afterload (6 kPa in systemic arteries, 2 kPa in pulmonary artery). Preload pressure was adjusted by raising the filling pressure column to provide a cardiac output of 30 ml min^{-1}, which was recorded using flow-through ultrasonic probes (4NRB; Transonic System) in the outflow lines and connected to a Transonic T206 flow meter. The composition of the Ringer's solution was 95 mmol l^{-1} NaCl, 30 mmol l^{-1} $NaHCO_3$, 1 mmol l^{-1} NaH_2PO_4, 2.5 mmol l^{-1} KCl, 1 mmol l^{-1} $MgSO_4$, 2 mmol l^{-1} $CaCl_2$, and 5 mmol l^{-1} glucose (Joyce et al., 2016). In this setting, the python heart beats spontaneously for hours. ECGs and local electrograms were recorded as previously described for anesthetized pythons. Once instrumented, the mid-section of the snake, encompassing the heart, was cut out and placed in an organ bath containing 9 g $liter^{-1}$ NaCl solution. The organ bath and Ringer's solution reservoir were water-jacketed and connected to a recirculating water heating system to allow simultaneous control of perfusate and bath temperature for heating from room temperature (20°C) to 35°C. Approximately 1 h passed from when the preparation was placed in the organ bath to when satisfactory instrumentation and quality of recording had been achieved. We then initiated the heating from 20°C to 35°C, which took 65 min. Thereafter, noradrenaline was added to the Ringer's solution perfusate to reach a final concentration of 1 µM.

Intra-arterial injections in eight awake pythons

We used eight adult ball pythons (*P. regius*) that were purchased, housed, and kept as above. Average body mass was 973 ± 63 g. Snakes were fasted at least 3 wk before experiments. Initial anesthesia, intubation, and ventilation followed the protocol described above.

To place the arterial catheter and ECG electrodes, each snake was anesthetized in a sealed container with isoflurane (IsoFlo Vet 100%; Orion Pharma Animal Health AS). After ∼15 min, the snakes were intubated endotracheally with soft polyethylene (made from pipettes; Sarstedt AG & Co.) for mechanical ventilation (Anesthesia Workstation; Hallowell EMC) with a mixture of oxygen and isoflurane (Fluotec Mark 3 vaporizer; Simonsen & Well A/S) at ∼200 ml min^{-1} $^{-1}$ kg^{-1} (4 breaths min^{-1}) and a maximum airway pressure at 15 cm H_2O (Jakobsen et al., 2017). Initially 5% isoflurane was given until full reflexes were lost, and then the supply was reduced to 2%. Body temperature was maintained at 29–31°C by a heating pad (Melissa Electric Heating Pad 631–109; Adexi A/S). A 6-cm-long incision anterior to the heart allowed for a catheter (Portex; Fine Bore Polythene Tubing; 0.58 mm ID 0.96 OD; Smiths Medical ASD) to be inserted in the vertebral artery to measure arterial blood pressure and to inject pharmaca. The catheter was fastened with a silk suture (Kruuse sutures; EP, 3.5), and the incision was closed with a monofilament suture (3–0; Ethilonx11).

Three stainless steel electrodes were placed subcutaneously on the back of the snakes, arranged in a lead II formation, measuring from right front to left back. One electrode was placed ∼2 cm in front of the heart to the right, and the other was placed ∼2 cm behind the heart to the left. The third reference electrode was placed in front of the heart on the opposite side of the front electrode. The electrodes were fastened ventrally with two stitches using a monofilament suture (3–0; Ethilonx11). Snakes were allowed to recover for 24 h at 30°C after surgery. During measurements, snakes were placed in boxes within a climate chamber at 30°C. The bottom of the boxes was covered with tin foil to ground the recordings. A transparent lid allowed filming of the snakes (Trendnet TV-IP572WI camera; Chania). Snakes were left undisturbed in the chamber throughout measurements. The ECG was amplified using a custom-built preamplifier and recorded in AcqKnowledge 3.9.1 (Biopac Systems, Inc.). To measure blood pressure, the catheter was connected to a pressure transducer (PX600; Baxter Edwards) that was calibrated daily against a static water column. For injections, the catheter was briefly disconnected, 5 µg kg^{-1} adrenaline or isoproterenol was infused (with at least 30 min between injections or when HR and mean arterial blood pressure had returned to normal levels), and the catheter was reconnected to the pressure transducer. The ECG signals were amplified by an in-house built preamplifier and recorded with a Biopac MP100 data acquisition system (Biopac Systems, Inc.) at 200 hz. The ECG traces were analyzed in LabChart 8. All snakes were euthanized upon completion of the measurements with an intra-arterial injection of 200 mg kg^{-1} pentobarbital (Euthasol vet 400 mg ml^{-1}; Virbac Denmark A/S).

Intra-arterial injections in six anesthetized pythons

We used six more ball pythons (*P. regius*) that were bought and housed as above. All snakes appeared healthy and fed regularly before the study. Average body mass was 707 ± 296 g (± SD). Snakes were fasted at least 7 d before experiments and none were shedding. All snakes received initial anesthesia by being placed in a box with 1 ml isoflurane per liter of air. Once reflexes to pinching had ceased, we injected 0.3 ml of 20 mg ml^{-1} lidocaine hydrochloride as local anesthetic at the site of incision for tracheotomy and catheterization. All snakes were

tracheotomized for ventilation, which was ∼500 ml of air min^{-1}. Air was delivered via a pressure cycling ventilator (Vetronic SAV-4) with an end ventilation airway pressure 8 cm H_2O at a respiration rate of 4 with a 2/3 inspiratory/expiratory time. Continuous anesthesia was kept by 2% isoflurane. End-tidal CO_2 was monitored to guarantee efficacy of ventilation using Cardell Touch (Midmark) with an end-tidal gas analyzer (Massimo IRMA AX+), which was also used to monitor cloacal temperature and end-tidal CO_2. With the same setup, we monitored temperature with an electric thermometer that was calibrated against two fluid thermometers in baths of 22°C and 35°C. The thermometer was inserted through the esophagus to the region of the heart. All snakes had catheter with heparinized sterile saline (0.9% sodium chloride with 50 IU ml^{-1}; Heparin-LEO 5,000 IU ml^{-1}; CP Pharmaceuticals) in the vertebral artery, except python 1, which had the catheter in the left descending aorta (because the vertebral artery was too small to allow cannulation in this animal). The catheter was ID 0.68 mm polyethylene tubing tied in with 4.0 silk. In all snakes, an initial ECG recording was made with electrodes set up as described for the open chest experiments and illustrated in Fig. 2 B. Once a satisfactory ECG had been recorded, we injected 5 mg kg^{-1} propranolol injection delivered in a volume of 1 ml kg^{-1}. After 20 min, a temperature ramp was initiated that stopped at 35°C. The temperature was raised by turning on a heating pad below and one above the snake (as above). For each 1°C increase in body temperature, the heating pads were briefly turned off for the recording of traces with low noise. After 36°C was reached, an injection of 5 µg kg^{-1} isoproterenol was given in a volume of 0.5 ml kg^{-1}, and the ECG was recorded for ∼5 min after injection.

Statistical analyses

All statistical analyses were made in SPSS (SPSS Statistics 25; IBM). Variables are presented as mean ± SEM. Comparisons are made using ANOVA and paired *t* tests with $P < 0.05$ considered significant (Fig. 4 D, linear regression analysis; Fig. 5, A and B, paired *t* tests; Fig. 6 A, one-way repeated-measurements ANOVA; Fig. 6 D, paired *t* test). We compared the incidence of T-wave inversion after heating without (Fig. 3) and with propranolol (Fig. 6 D) using a χ^2 test. The effect of heating on HR in the presence and absence of propranolol was determined using a two-way repeated-measurements ANOVA (fixed factor: presence of propranolol, repeated factor: temperature).

Online supplemental material

Fig. S1 shows T-wave inversion in the ECG upon noradrenaline administration recorded from an ex vivo perfused heart. Fig. S2 shows scatter plots between expression levels versus log2fold change. Table S1 lists the ECG intervals during, before, and after heating in the presence of propranolol.

Results

Increase in body temperature causes change in T-wave polarity

To investigate whether change in body temperature causes change in T-wave polarity in ectotherms, we recorded body surface ECGs of five anesthetized pythons during heating from ∼25 to 35°C. Fig. 2 A shows an example of the change in temperature during the heating with the arrows indicating the moments when an ECG was recorded from locations as indicated in Fig. 2 C. The T-wave was negative in lead I in four pythons and positive in one. During heating, HR increased and the PR, QRS, and QT intervals shortened (Table 1). In all five pythons, the T-wave polarity inverted as thoracic temperature increased, whereas QRS polarity did not change. The change in polarity of the T-wave was not always visible in each lead. Fig. 3 A shows an ECG of a python where the T-wave in lead I became more negative upon heating, while in aVF its polarity changed from negative to positive. Reconstruction of the vector cardiogram based on these leads shows that the electrical vector before heating (blue) was above the x axis and after heating (red) below the x axis (Fig. 3 B), indicating a negative and positive T-wave in aVF, respectively. The change in dominant electrical vector of the T-wave upon heating differed markedly between pythons (Fig. 3 C). The wave inversion occurred most often in lead III and aVF (three out of five; Table 1). These findings suggest that change in T-wave polarity upon heating is intrinsic to all hearts, but the detection of such changes depends on the electrocardiographic lead.

Local activation and repolarization patterns during heating

While recording the ECGs, we simultaneously recorded epicardial electrograms (open-chest) in order to relate the T-wave inversion to local activation and repolarization patterns (Fig. 4 A). The timing of activation was earlier at the base than at the apex and occurred on average 47 ± 6 ms versus 85 ± 7 ms, respectively, after the onset of the QRS complex. There was no change to the pattern of ventricular activation during heating, but total activation time decreased, leading to a shorter QRS duration (Table 1). In heated hearts, the ventricular base activated on average at 33 ± 4 ms and the apex at 58 ± 7 ms after the onset of the QRS complex.

At room temperature, full repolarization was reached earlier in the right side of the ventricle than in the left side in four pythons (829 ± 114 ms versus 908 ± 137 ms; $P = 0.048$), whereas in one python, this was opposite (1,116 ms versus 993 ms, respectively). It was this individual that showed a positive T-wave in lead I. Upon heating, repolarization shortened (Fig. 4 B) on average by 322 ± 76 ms, giving rise to shorter QT intervals. The dominant electrical vector based on local repolarization gradients changed during heating in each python. Fig. 4 C shows a repolarization map before (upper) and after (lower) heating of the same python as in Fig. 3, A and B. Note that the change in electrical vector based on local repolarization corresponds to the change in dominant electrical vector based on the T-wave in the ECG. The change in local repolarization gradients upon heating was different across pythons but correlated significantly with the change in T-wave vector (Fig. 4 D).

Catecholaminergic stimulation, but not temperature, is sufficient to change T-wave polarity

To investigate whether increasing body temperature alone was sufficient to change T-wave polarity, we recorded an ECG from a single decapitated snake that had its central cardiovascular

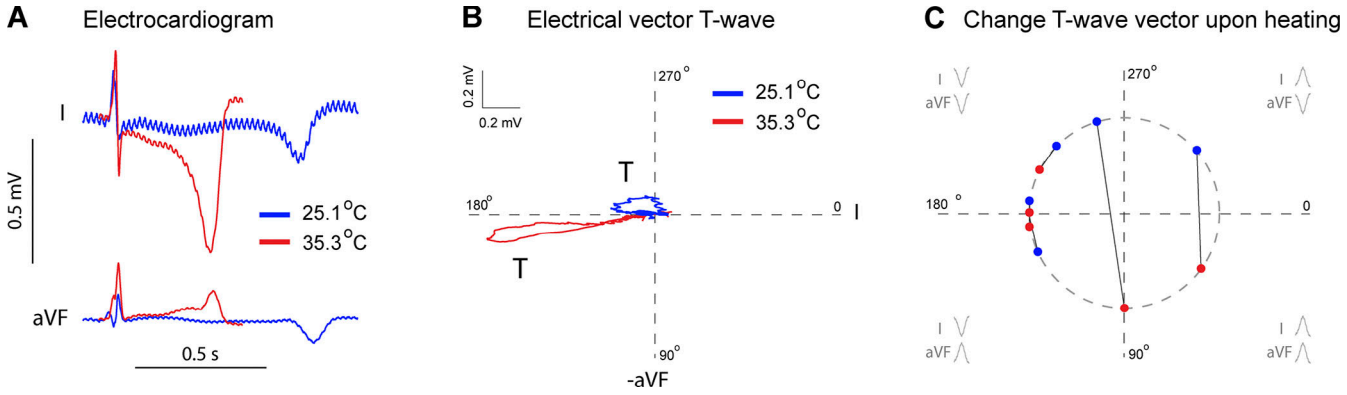

Figure 3. **Detection of T-wave inversion is dependent on the ECG lead. (A)** In python 1, in the course of heating from 25.1°C (blue) to 35.2°C (red), the T-wave inverted in lead aVF (bottom traces) but not in lead I (top traces). **(B)** A vector cardiogram of the T-wave before and after heating. **(C)** A graph showing the T-wave vector based on lead aVF and lead I before (blue dot) and after heating (red dot) for pythons 1-5.

system perfused with Ringer's solution. When the temperature was raised from room temperature to ∼39.5°C, the HR increased, and PR and QT intervals shortened. The T-wave, however, did not change polarity as in the anesthetized snakes with intact cardiovascular and nervous systems (Fig. S1 A). To simulate the autonomic nervous system activity, we added noradrenaline, a β-adrenergic receptor agonist, to the Ringer's solution to reach a final concentration of ∼1 µM and recorded a pronounced T-wave inversion within 1 min (Fig. S1 A). This observation suggested an important role of β-adrenergic receptor stimulation in T-wave inversion during heating. To investigate this further, we recorded ECGs in eight awake and undisturbed pythons that were kept at a stable temperature before and after β-adrenergic receptor stimulation (Table 2). First, we gave an intra-arterial injection of saline and saw no effect on any ECG parameter. Adrenaline caused change in T-wave polarity in seven out of eight snakes (Fig. 5 A). The inversion lasted a few minutes typically and progressed from the normal discordant relative to the R, to flat (or no T-wave), to concordant with a progressively greater amplitude, and then a reversal back to discordant. Injections of isoproterenol, a β-adrenergic receptor agonist, induced T-wave inversion of long duration (10s of minutes) in all eight pythons (Fig. 5 B). These findings show that β-adrenergic stimulation by catecholamines is sufficient for inducing changes in T-wave polarity and could explain T-wave inversion during heating.

Blockade of β-receptors by propranolol prevents T-wave inversion during heating

We then hypothesized that change in T-wave polarity during heating would not occur in the absence of β-adrenergic stimulation. To test this hypothesis, we administered intravenously 5 mg kg^{-1} propranolol, a β-adrenergic receptor blocker, to six anesthetized pythons during continuous ECG recording (Table S1). During heating from 25°C to 36°C, propranolol did not prevent HR increase (24 ± 2 to 47 ± 5 bpm; P = 0.003), but it prevented any further rise in HR upon injection of the β-adrenergic receptor agonist isoproterenol (47 ± 5 versus 46 ± 3 bpm; P = 0.67). The latter indicates that administration of propranolol provided full blockade of the β-adrenergic receptors. All pythons showed a positive T-wave in lead I after propranolol administration. In five out of six pythons, the polarity of the T-wave did not change during heating or after administration of isoproterenol (Fig. 6, B and C). In one out of six pythons, T-wave inversion did occur both in lead I and lead aVF. This python also

Table 1. **Changes in ECG parameters upon heating in individual pythons measured with open chest**

	HR (bpm)		PR (ms)		QRS (ms)		QT (ms)		T-wave inversion	
	25°C	36°C	25°C	36°C	25°C	36°C	25°C	36°C	In lead	At (°C)
Python 1	35	96	319	132	72	58	1,271	475	aVF	27
Python 2	55	118	769	351	108	49	822	380	II	28
Python 3	30	65	485	226	96	70	931	515	All leads	33
Python 5	22	32	593	394	122	100	2,110	1,440	III	34
Python 6	34	73	339	212	93	51	1,391	362	III, aVF	34
Average (ms)	35	77[a]	501	263[a]	98	66[a]	1,305	634[a]		
SEM	6	15	84	48	8	9	227	203		

Pythons were heated from 25°C (before) to 35°C (after). The T-wave inversion column shows the leads in which the T-wave inverted and the temperature when this occurred.
[a]P < 0.05, paired *t* test.

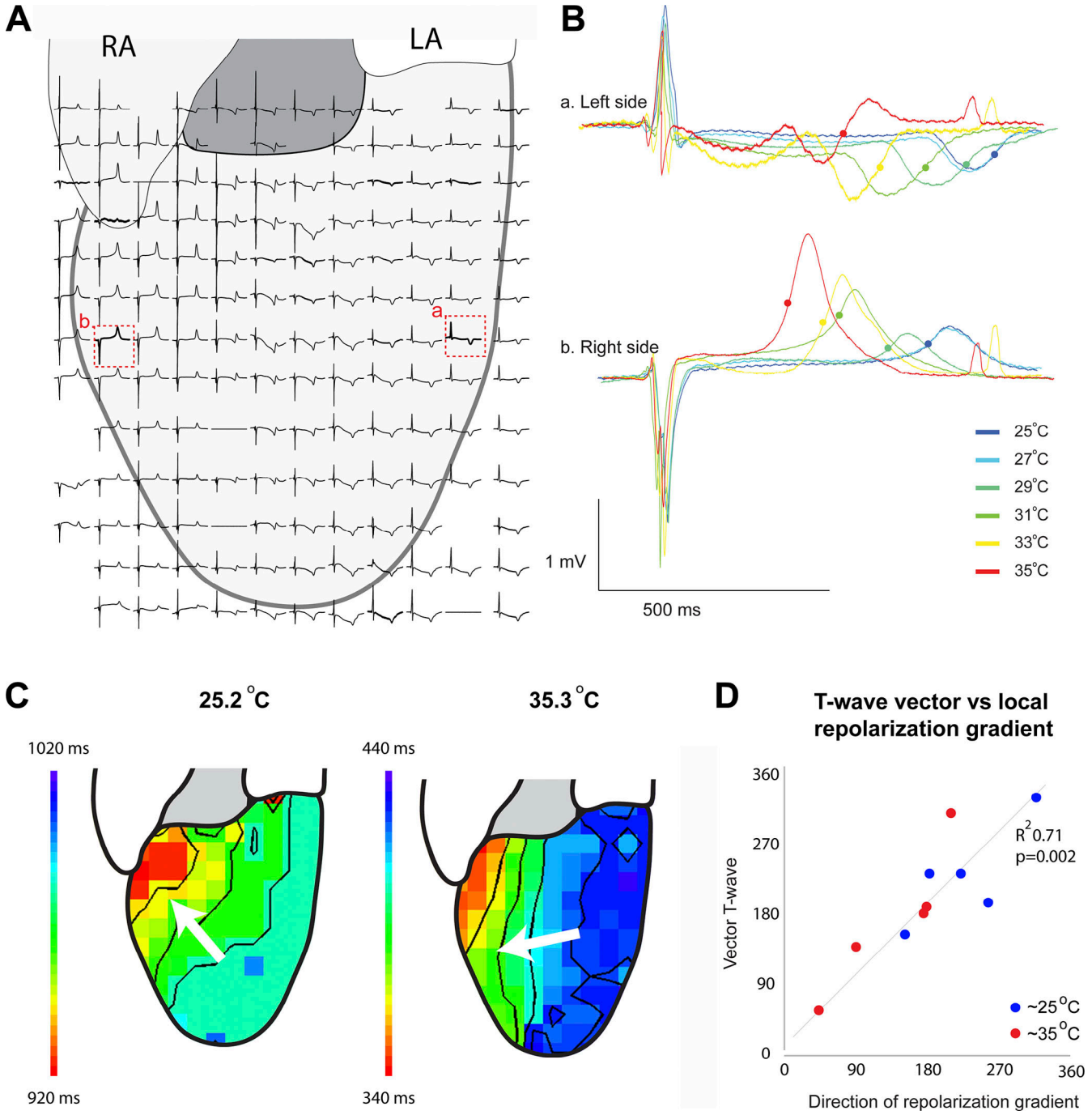

Figure 4. **Determining local epicardial repolarization patterns using open-chest mapping during heating. (A)** Schematic representation of a python heart with superimposed local electrograms recorded with the multi-electrode grid. **(B)** Local electrograms from the left (a) and right (b) sides of the ventricle at different temperatures. Note that the time to repolarization (indicated by the solid circle) shortens upon heating. **(C)** Repolarization maps before (left) and after (right) heating showing the change in repolarization sequence. **(D)** Scatter diagram showing the correlation between the direction of the repolarization gradient and the electrical vector of the T-wave (n = 5). LA, left atrium; RA, right atrium.

developed arrhythmias by first exhibiting T-wave alternans at 34.4°C, and after administration of isoproterenol, it developed ventricular premature beats (Fig. 6 E). Taken together, the incidence of T-wave inversion upon heating was significantly lower after β-blockade with propranolol when compared with the control pythons (Fig. 3; one out of six versus five out of five, respectively; P = 0.0057; χ^2), indicating that it is not changes to body temperature per se, but increased sympathetic tone, that underlies the change in T-wave polarity.

Gene expression analysis of the ventricle reveals regional differences and evolutionary conservation

Next, we aimed at relating heterogeneity in repolarization and change in T-wave polarity to heterogeneity in gene expression.

Table 2. **Changes in ECG parameters induced by catecholamines in awake pythons (*n* = 8)**

	Heart rate (bpm)		PR (ms)		QRS (ms)		QT (ms)	
Adrenaline								
Before	19	2	648	27	93	7	1,698	141
After	31	5[a]	549	44[a]	104	8	1,406	131[a]
Isoproterenol								
Before	17	1	655	32	94	6	1,792	100
After	50	5[a]	452	45	91	4	1,036	123[a]

[a]P < 0.05, paired *t* test.

We collected transmural ventricular tissue samples from the left and the right side and performed RNA sequencing (Fig. 7 A). We found 428 genes to be more abundantly expressed in the left side and 161 in the right side of the ventricle (P adjusted < 0.05; Fig. 7, B and C). In addition, we performed a hierarchical cluster analysis based on differentially expressed genes using a P adjusted value <0.1, which resulted in four separate groups of genes (Fig. 7 D). For each group, we investigated enrichments for KEGG pathways (Kanehisa et al., 2012). Among various pathways, we found genes related to "cardiac muscle contraction" to be enriched in the left side (Fig. 7 E), which is the side with the greater systolic blood pressure. In the right side, we found genes related to "adrenergic signaling in cardiomyocytes" and "calcium signaling pathway" to be enriched. At a single-gene level, we found several genes encoding proteins involved in calcium current (e.g., *Cacna1g* and *Cacna2d2*) to be differentially expressed. These findings suggest that gene expression may underlie some of regional differences in repolarization and the sensitivity to adrenergic stimulation.

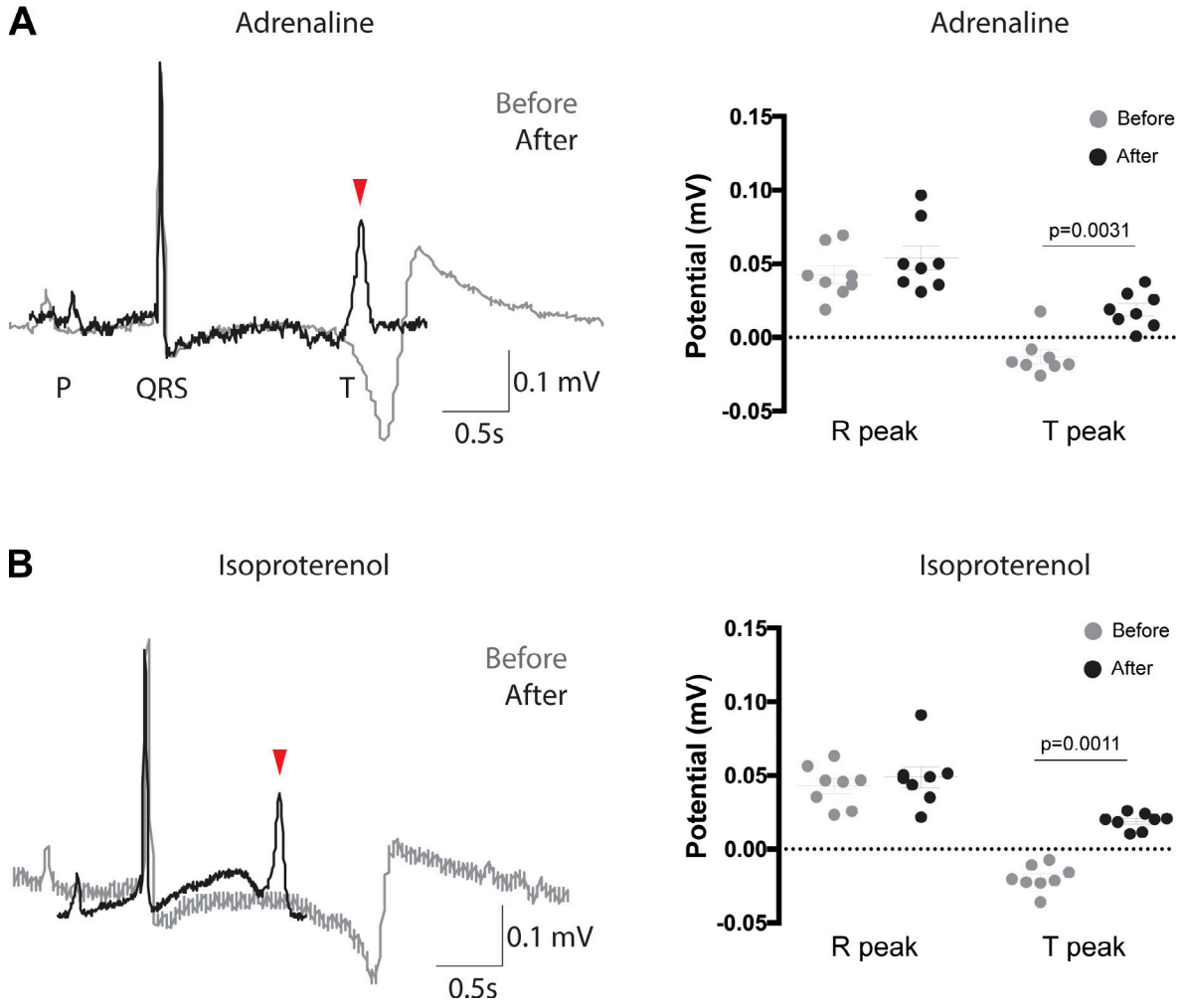

Figure 5. **Catecholaminergic stimulation is sufficient to cause T-wave inversion. (A)** In awake and undisturbed pythons (*n* = 8), the intra-arterial administration of adrenaline (5 µg kg^{-1}) had no effect on the R amplitude, but caused inversion of the T-wave in seven animals. **(B)** In awake and undisturbed pythons (*n* = 8), the intra-arterial administration of isoproterenol 5 µg kg^{-1}, a β-adrenergic agonist, had no effect on the R amplitude, but caused a substantial shortening of the time to repolarization and an inversion of the T-wave in all animals.

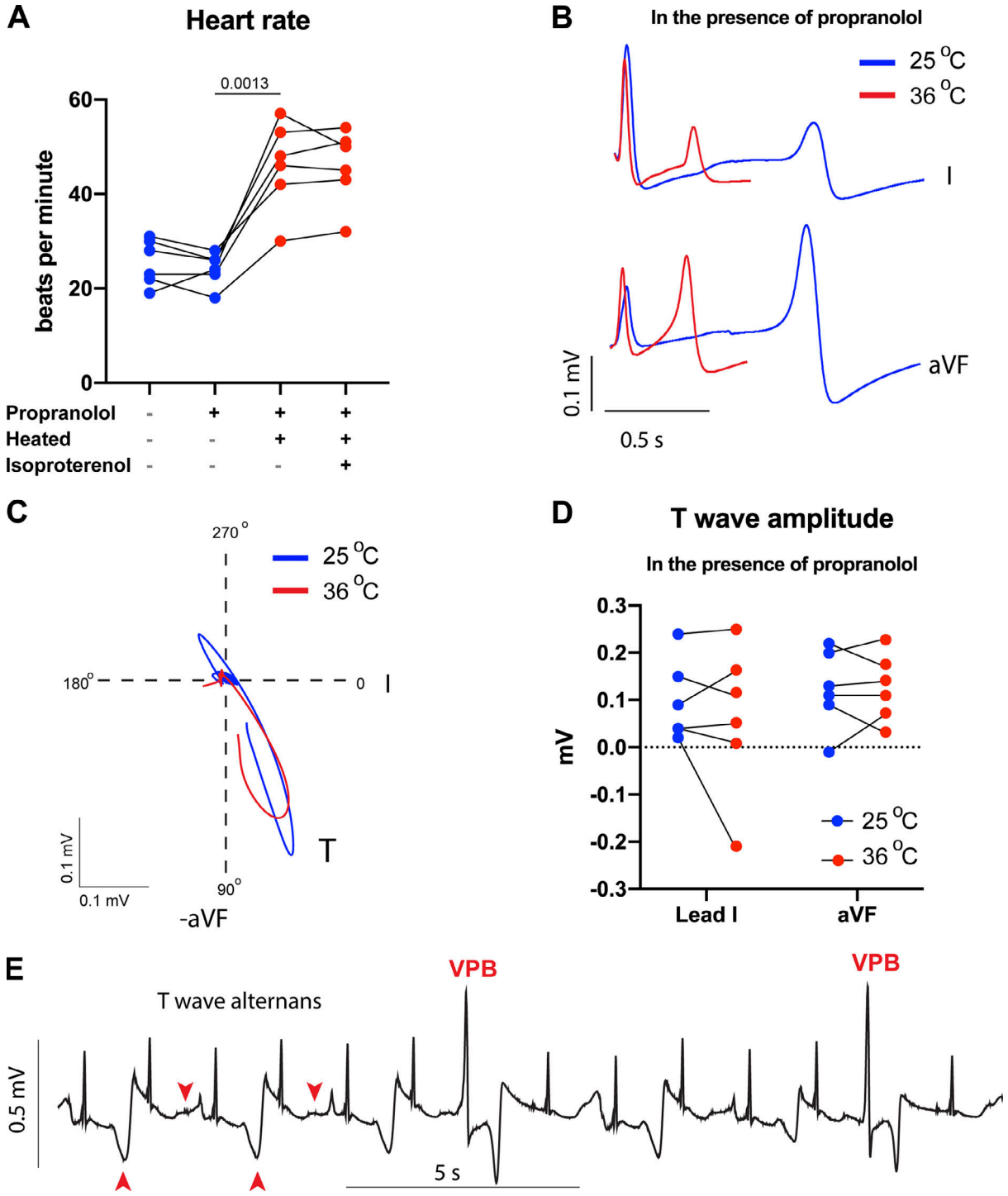

Figure 6. **β-Adrenergic receptor blockade prevents T-wave inversion during heating. (A)** The bar graph shows changes in HR upon first propranolol (5 mg kg^{-1}) administration, then heating to 36°C, and finally isoproterenol (5 µg kg^{-1}) administration. HR increased significantly during heating (ANOVA [repeated measurements], P = 0.0013). **(B)** Example of lead I (upper) and lead aVF (lower) before and after heating in the presence of propranolol. **(C)** Example of vector cardiogram before and after heating in the presence of propranolol. **(D)** Bar graph showing the amplitude of the T-wave in lead I and aVF before (blue dots) and after (red dots) heating. T-wave amplitude did not change upon heating in lead I and aVF (paired *t* test; P = 0.43 and P = 0.56, respectively). **(E)** Python 16 exhibited ventricular premature beats (VPBs), which was preceded by T-wave alternans (examples are indicated with red arrowheads).

We did detect *Scn5a*, encoding the cardiac sodium channel, and *Kcnq1* and *Kcnh6*, encoding major repolarizing channels, but those genes were not differentially expressed between the left and right side of the ventricle (Fig. S2 A). Moreover, genes encoding transcription factors required for ventricular development, e.g., *Gata4*, *Hey2*, *Hand2*, *Tbx5*, and *Tbx20*, were homogeneously expressed. We also detected expression of *Adrb1* and *Adora2a*, which are receptors for noradrenaline

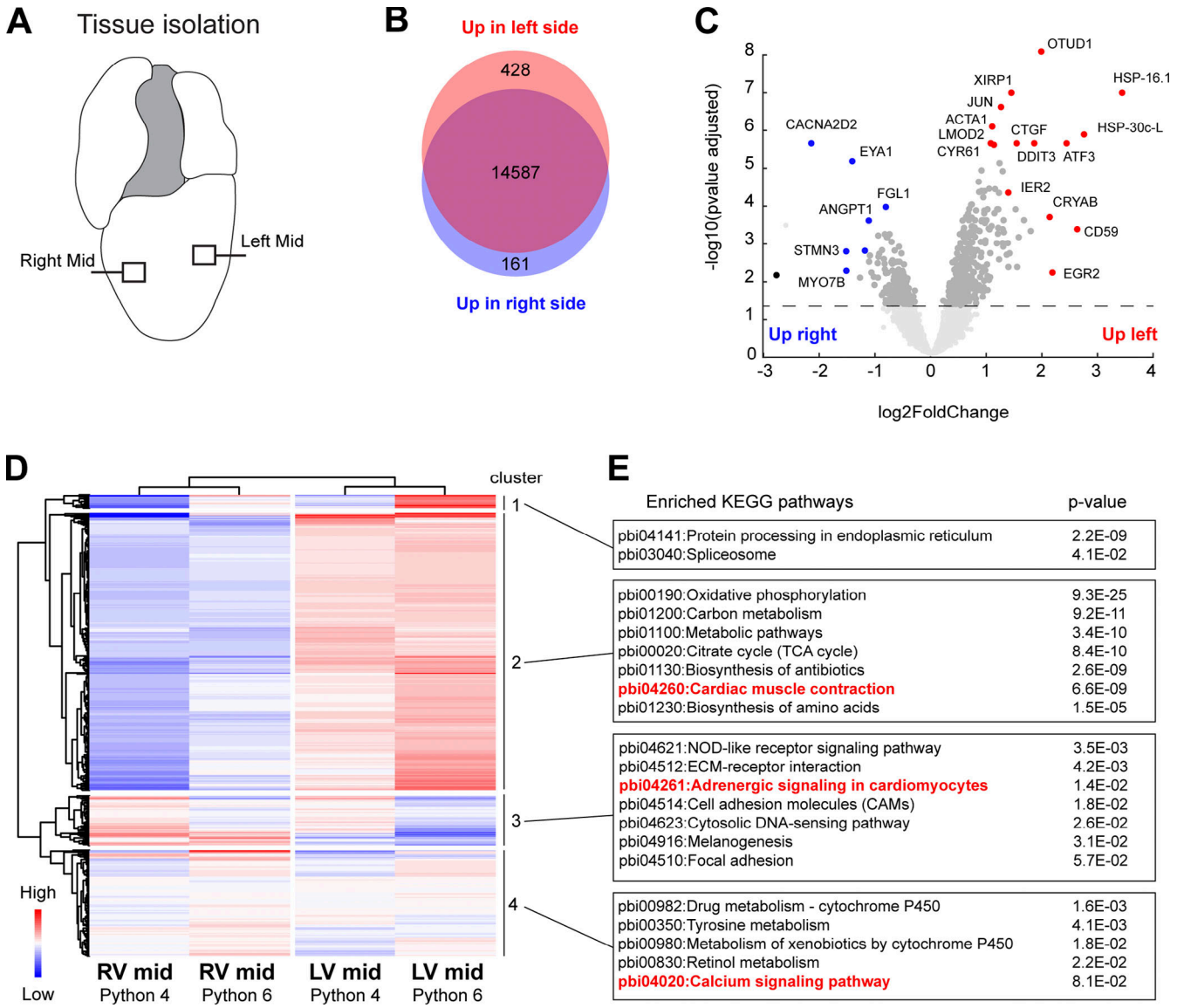

Figure 7. **Gene expression analysis of the python ventricle. (A)** The location from which tissue was collected (ventral side). **(B)** Diagram indicating the enrichment of genes in either the right or left side of the ventricle. **(C)** Scatter plot showing for each gene the statistical significance on the y axis and the magnitude of change on the x axis. **(D)** A heat map showing four clusters of the relative expression of genes between the right and left side of the ventricle. **(E)** KEGG pathway analysis for each of the four clusters. LV, left ventricle; Mid, mid ventricle; RV, right ventricle.

and adenosine, respectively (Fig. S2 B). In aggregate, the gene expression analysis reveals that the python myocardium is likely formed and maintained by numerous evolutionarily conserved mechanisms.

Discussion

Our data show that, in pythons, local repolarization gradients change when body temperature increases, causing altered T-wave shape and even change in polarity. We show here, however, that temperature does not change patterns of repolarization if the β-adrenergic receptors are blocked. We therefore propose that catecholamines, likely released from sympathetic neurons or potentially acting as hormones, are the link between the previously observed changes in body temperature and T-wave inversion. This resembles the modulating role of catecholamines on repolarization in mammals and indicates an evolutionary conserved mechanism.

For ventricular repolarization of pythons to be similar to that of mammals, our study suggests that at least three conditions have to be met. First, there should be evolutionary conservation of the electrophysiological processes, and our RNA sequencing demonstrates a substantial evolutionary conservation on the transcript level, including of the major ion-handling channels, in agreement with previous studies (Olson, 2006; Castoe et al., 2013; Duan et al., 2017; Filatova et al., 2021; Offerhaus et al., 2021). Second, catecholamines should augment differences in repolarization time between regions within the ventricle, and we find this to be the case in pythons. Third, there should be a clear left–right difference in the timing of repolarization, and we

show here that it is in this feature that the pythons, and likely other reptiles, can differ substantially from mammals.

The onset of repolarization depends on local action potential duration and the moment of local activation relative to the onset of the QRS complex. In mammals, activation starts simultaneously in the left and right ventricles through activation via the ventricular conduction system (Durrer et al., 1970), whereas in pythons, we show here that ventricular activation resembles the primitive base-to-apex pattern (Gregorovicova et al., 2018). Furthermore, in pythons, the pronounced difference in systolic blood pressure between the left and right sides (Wang et al., 2003) is not mirrored by substantially late repolarization in the left ventricle, again in contrast with mammals. Thus, while we can report evolutionary conservation of catecholamines as key modulators of ventricular repolarization patterns, the differences in ventricular activation pattern and local action potential durations account for much of the divergence in ventricular repolarization between pythons and mammals.

Using KEGG pathway analysis, we discovered various pathways that are found in humans as well (Kanehisa et al., 2012), including enrichment of genes involved in β1-adrenergic signaling at the right side of the ventricle. Although it is unclear how this enrichment is related to the T-wave inversion during heating, the detection of these transcripts strongly suggests an evolutionarily conserved mechanism of autonomic modulation of cardiac function between mammals and pythons, and by extension, reptiles. The gene expression analysis also showed evolutionary conservation of molecular determinants of repolarization by showing expression of cardiogenic transcription factors and their downstream target genes in the heart, including ion channels handling sodium, calcium, and potassium ions. These genes are also expressed in the hearts of mammals and have been found in ectotherms before (Duan et al., 2017; Castoe et al., 2013; Olson, 2006). This evolutionary conservation was further supported by the expression of many genes involved in the synthesis and reception of catecholamines, which in mammals are well-known modulators of ventricular repolarization (Sparks et al., 1970; Yagishita et al., 2015).

T-wave inversion is related to augmented left–right differences in repolarization, of which the underlying mechanism is unknown. The presence of rapid delayed rectifier potassium current and L-type calcium current have been demonstrated in cardiomyocytes from the Burmese python (Abramochkin et al., 2020). These currents are important for ventricular repolarization in mammals, and L-type calcium current is modulated by adrenergic stimulation (Kass and Wiegers, 1982; Volders et al., 2003; Meijborg et al., 2020). Expression analysis did not reveal left–right differences with regards to catecholaminergic synthesis and receptor pathways, which is consistent with previous data suggesting similar sensitivity to adrenergic stimulation in myocardial preparations from the left and right sides of the ball python heart (Zaar et al., 2007). On the other hand, the KEGG pathway analysis suggests greater impact of adrenergic stimulation on the right than the left side of the ventricle. The abundant expression of the adrenergic receptor *Adrb1* is consistent with a recent pharmacological investigation suggesting the β1-adrenergic receptor is the dominant subtype expressed in snake myocardium (Abraham et al., 2019). Although our data suggest evolutionary conservation of adrenergic signaling, the sensitivity of the ventricular myocardium for subtypes of β-adrenergic receptors may differ across ectotherms (Skeberdis et al., 1997).

We also detected *Tbx5*, which is expressed more in the left ventricle than in the right ventricle in animals with a full ventricular septum, namely crocodilians, birds, and mammals (Takeuchi et al., 2003; Bruneau et al., 2001; Jensen et al., 2018). Pythons and monitor lizards are the only known groups of vertebrates with a functional pressure separation of the ventricle while a full ventricular septum is absent (Burggren and Johansen, 1982). In neither group is *Tbx5* expressed at greater levels on the left side of the ventricle. This observation supports the notion that *Tbx5* is an ambiguous marker of ventricular septation in animals with a partial septum (Poelmann and Gittenberger-de Groot, 2019; Hanemaaijer et al., 2019).

The T-wave reflects a vulnerable window for the occurrence of arrhythmias. During this window, part of the heart is still refractory (late repolarization, end T-wave), whereas other parts are not (early repolarization, start T-wave). Accordingly, an ectopically originated activation front during this window may encounter refractory myocardium, which sets the stage for conduction block and the onset of reentrant arrhythmias. This phenomenon is clinically known as the R-on-T phenomenon (Smirk, 1949) and illustrates the relevance of gradients in repolarization for arrhythmogenesis (Boukens et al., 2016). Beat-to-beat changes in T-wave polarity, i.e., T-wave alternans, also predispose to arrhythmias, as seen in acute ischemia (Janse et al., 1980) or in the time period preceding ventricular fibrillation (Pastore et al., 1999). We observed premature ventricular beats in one python that occurred after T-wave alternans. The premature beats likely originated in the ventricular working myocardium as a ventricular conduction system is not present in ball pythons. In several species of mammals, including humans, stellate ganglion stimulation shortens repolarization heterogeneously in the heart, thereby changing T-wave polarity in the ECG (Schwartz and Malliani, 1975; Kuo and Surawicz, 1976; Meijborg et al., 2020). We show that β-adrenergic stimulation is sufficient to induce similar changes in the T-wave, including inversion, in awake pythons. Whether the catecholamines that induce changes to repolarization are released by nerves in the heart under control of stellate-like ganglia in pythons is unknown at this point. Alternatively, catecholamines of the peripheral nervous system could be released into the bloodstream, a mechanism that has been shown in the ectothermic rainbow trout during warming (Currie et al., 2013).

The physiological significance of the manner in which temperature affects repolarization in the python heart remains elusive. In ectotherms, the rise in metabolism with elevated body temperature (Fry and Hart, 1948; Fobian et al., 2014) requires higher cardiac output, and our data show that although the HR elevations in response to heating were not different ($P = 0.07$), there was a considerably lower absolute HR at 36°C upon sympathetic blockade (47 ± 5 bpm versus 77 ± 15 bpm, respectively; $P = 0.05$). The latter could indicate that increase in autonomic tone is required for reaching sufficient cardiac output

needed at higher body temperatures in ectotherms. The occurrence of T-wave inversions during high sympathetic tone may be a "bystander effect" and related to heterogeneous sensitivity of the myocardium to β-adrenergic stimulation. In mammals, such as humans and pigs, increased autonomic tone via stellate ganglia stimulation also causes T-wave inversions and sets the stage for ventricular premature beats and arrhythmias similar to what we observed in one of the six pythons treated with both propranolol and isoproterenol. Whether changes in repolarization in pythons upon heating enhance cardiac performance, for example when body temperature increases during basking in the sun, remains to be studied in recovered animals performing natural behavioral thermoregulation.

Conclusion

Previous reports associated T-wave changes in reptiles to changes in body temperature. Our data, however, show that temperature itself does not change the direction of the repolarization gradient. Instead, a rise in body temperature increases the sympathetic tone on the heart, which then modulates the direction of the repolarization gradient. This shows that the autonomic nervous system is a key modulator of ventricular repolarization in pythons that resembles the situations in mammals. Moreover, we show substantial evolutionary conservation on the transcript level of key ion channels and catecholamine synthesis and reception.

Acknowledgments

David A. Eisner served as editor.

We thank Rasmus Buchanan, Heidi Meldgaard, and Karel van Duijvenboden for technical assistance.

B.J.D. Boukens was supported by the Dutch Heart Foundation (2016T047). W. Joyce is supported by a Novo Nordisk Foundation grant (NNF19OC0055842), and T. Wang was supported by the Danish Council for Independent Research/Natural Sciences.

The authors declare no competing financial interests.

Author contributions: B.J.D. Boukens, W. Joyce, T. Wang, and B. Jensen designed the research; B.J.D. Boukens, W. Joyce, D.L. Kristensen, I. Hooijkaas, T. Wang, and B. Jensen performed experiments; B.J.D. Boukens, W. Joyce, D.L. Kristensen, A. Jongejan, T. Wang, and B. Jensen analyzed data; and B.J.D. Boukens, W. Joyce, T. Wang, and B. Jensen wrote the paper. All authors approved the final version of the manuscript.

Submitted: 15 September 2020
Revised: 28 October 2021
Accepted: 19 November 2021

References

Abraham, G., S. Hoffmann, I. Hochheim, and M. Pees. 2019. Distribution and properties of cardiac and pulmonary β-adrenergic receptors in corn snakes (Pantherophis guttatus) and Boa constrictor (Boa constrictor). *Comp. Biochem. Physiol. A Mol. Integr. Physiol.* 233:17–23. https://doi.org/10.1016/j.cbpa.2019.03.023

Abramochkin, D.V., V. Matchkov, and T. Wang. 2020. A characterization of the electrophysiological properties of the cardiomyocytes from ventricle, atrium and sinus venosus of the snake heart. *J. Comp. Physiol. B.* 190:63–73. https://doi.org/10.1007/s00360-019-01253-5

Anders, S., P.T. Pyl, and W. Huber. 2015. HTSeq--a Python framework to work with high-throughput sequencing data. *Bioinformatics.* 31:166–169. https://doi.org/10.1093/bioinformatics/btu638

Bolger, A.M., M. Lohse, and B. Usadel. 2014. Trimmomatic: a flexible trimmer for Illumina sequence data. *Bioinformatics.* 30:2114–2120. https://doi.org/10.1093/bioinformatics/btu170

Boukens, B.J., R. Walton, V.M. Meijborg, and R. Coronel. 2016. Transmural electrophysiological heterogeneity, the T-wave and ventricular arrhythmias. *Prog. Biophys. Mol. Biol.* 122:202–214. https://doi.org/10.1016/j.pbiomolbio.2016.05.009

Boukens, B.J.D., D.L. Kristensen, R. Filogonio, L.B.T. Carreira, M.R. Sartori, A.S. Abe, S. Currie, W. Joyce, J. Conner, T. Opthof, et al. 2019. The electrocardiogram of vertebrates: Evolutionary changes from ectothermy to endothermy. *Prog. Biophys. Mol. Biol.* 144:16–29. https://doi.org/10.1016/j.pbiomolbio.2018.08.005

Bruneau, B.G., G. Nemer, J.P. Schmitt, F. Charron, L. Robitaille, S. Caron, D.A. Conner, M. Gessler, M. Nemer, C.E. Seidman, and J.G. Seidman. 2001. A murine model of Holt-Oram syndrome defines roles of the T-box transcription factor Tbx5 in cardiogenesis and disease. *Cell.* 106:709–721. https://doi.org/10.1016/S0092-8674(01)00493-7

Burdon-Sanderson, J. 1880. On the Time-Relations of the Excitatory Process in the Ventricle of the Heart of the Frog. *J. Physiol.* 2:384–435. https://doi.org/10.1113/jphysiol.1880.sp000070

Burggren, W.W., and K. Johansen. 1982. Ventricular Haemodynamics in the Monitor Lizard Varanus Exanthematicus: Pulmonary and Systemic Pressure Separation. *J. Exp. Biol.* 96:343–354. https://doi.org/10.1242/jeb.96.1.343

Castoe, T.A., A.P.J. de Koning, K.T. Hall, D.C. Card, D.R. Schield, M.K. Fujita, R.P. Ruggiero, J.F. Degner, J.M. Daza, W. Gu, et al. 2013. The Burmese python genome reveals the molecular basis for extreme adaptation in snakes. *Proc. Natl. Acad. Sci. USA.* 110:20645–20650. https://doi.org/10.1073/pnas.1314475110

Corbin-Leftwich, A., H.E. Small, H.H. Robinson, C.A. Villalba-Galea, and L.M. Boland. 2018. A *Xenopus* oocyte model system to study action potentials. *J. Gen. Physiol.* 150:1583–1593. https://doi.org/10.1085/jgp.201812146

Currie, S., E. Ahmady, M.A. Watters, S.F. Perry, and K.M. Gilmour. 2013. Fish in hot water: hypoxaemia does not trigger catecholamine mobilization during heat shock in rainbow trout (Oncorhynchus mykiss). *Comp. Biochem. Physiol. A Mol. Integr. Physiol.* 165:281–287. https://doi.org/10.1016/j.cbpa.2013.03.014

Duan, J., K.W. Sanggaard, L. Schauser, S.E. Lauridsen, J.J. Enghild, M.H. Schierup, and T. Wang. 2017. Transcriptome analysis of the response of Burmese python to digestion. *Gigascience.* 6:1–18. https://doi.org/10.1093/gigascience/gix057

Durrer, D., R.T. van Dam, G.E. Freud, M.J. Janse, F.L. Meijler, and R.C. Arzbaecher. 1970. Total excitation of the isolated human heart. *Circulation.* 41:899–912. https://doi.org/10.1161/01.CIR.41.6.899

Filatova, T.S., D.V. Abramochkin, N.S. Pavlova, K.B. Pustovit, O.P. Konovalova, V.S. Kuzmin, and H. Dobrzynski. 2021. Repolarizing potassium currents in working myocardium of Japanese quail: a novel translational model for cardiac electrophysiology. *Comp. Biochem. Physiol. A Mol. Integr. Physiol.* 255:110919. https://doi.org/10.1016/j.cbpa.2021.110919

Fobian, D., J. Overgaard, and T. Wang. 2014. Oxygen transport is not compromised at high temperature in pythons. *J. Exp. Biol.* 217:3958–3961. https://doi.org/10.1242/jeb.105148

Fry, F.E.J., and J.S. Hart. 1948. The relation of temperature to oxygen consumption in the goldfish. *Biol. Bull.* 94:66–77. https://doi.org/10.2307/1538211

Galli, G., E.W. Taylor, and T. Wang. 2004. The cardiovascular responses of the freshwater turtle Trachemys scripta to warming and cooling. *J. Exp. Biol.* 207:1471–1478. https://doi.org/10.1242/jeb.00912

Gregorovicova, M., D. Sedmera, and B. Jensen. 2018. Relative position of the atrioventricular canal determines the electrical activation of developing reptile ventricles. *J. Exp. Biol.* 221:jeb178400. https://doi.org/10.1242/jeb.178400

Hanemaaijer, J., M. Gregorovicova, J.M. Nielsen, A.F.M. Moorman, T. Wang, R.N. Planken, V.M. Christoffels, D. Sedmera, and B. Jensen. 2019. Identification of the building blocks of ventricular septation in monitor lizards (Varanidae). *Development.* 146:dev.177121. https://doi.org/10.1242/dev.177121

Huang, W., B.T. Sherman, and R.A. Lempicki. 2009. Systematic and integrative analysis of large gene lists using DAVID bioinformatics resources. *Nat. Protoc.* 4:44–57. https://doi.org/10.1038/nprot.2008.211

Jakobsen, S.L., C.J.A. Williams, T. Wang, and M.F. Bertelsen. 2017. The influence of mechanical ventilation on physiological parameters in ball pythons (Python regius). *Comp. Biochem. Physiol. A Mol. Integr. Physiol.* 207:30–35. https://doi.org/10.1016/j.cbpa.2017.02.012

Janse, M.J., F.J. van Capelle, H. Morsink, A.G. Kléber, F. Wilms-Schopman, R. Cardinal, C.N. d'Alnoncourt, and D. Durrer. 1980. Flow of "injury" current and patterns of excitation during early ventricular arrhythmias in acute regional myocardial ischemia in isolated porcine and canine hearts. Evidence for two different arrhythmogenic mechanisms. *Circ. Res.* 47:151–165. https://doi.org/10.1161/01.RES.47.2.151

Jensen, B., A.F.M. Moorman, and T. Wang. 2014. Structure and function of the hearts of lizards and snakes. *Biol. Rev. Camb. Philos. Soc.* 89:302–336. https://doi.org/10.1111/brv.12056

Jensen, B., B.J. Boukens, D.A. Crossley II, J. Conner, R.A. Mohan, K. van Duijvenboden, A.V. Postma, C.R. Gloschat, R.M. Elsey, D. Sedmera, et al. 2018. Specialized impulse conduction pathway in the alligator heart. *eLife.* 7:e32120. https://doi.org/10.7554/eLife.32120

Joyce, W., M. Axelsson, J. Altimiras, and T. Wang. 2016. In situ cardiac perfusion reveals interspecific variation of intraventricular flow separation in reptiles. *J. Exp. Biol.* 219:2220–2227. https://doi.org/10.1242/jeb.139543

Kanehisa, M., S. Goto, Y. Sato, M. Furumichi, and M. Tanabe. 2012. KEGG for integration and interpretation of large-scale molecular data sets. *Nucleic Acids Res.* 40(D1):D109–D114. https://doi.org/10.1093/nar/gkr988

Kass, R.S., and S.E. Wiegers. 1982. The ionic basis of concentration-related effects of noradrenaline on the action potential of calf cardiac purkinje fibres. *J. Physiol.* 322:541–558. https://doi.org/10.1113/jphysiol.1982.sp014054

Kim, D., B. Langmead, and S.L. Salzberg. 2015. HISAT: a fast spliced aligner with low memory requirements. *Nat. Methods.* 12:357–360. https://doi.org/10.1038/nmeth.3317

Kuo, C.S., and B. Surawicz. 1976. Ventricular monophasic action potential changes associated with neurogenic T wave abnormalities and isoproterenol administration in dogs. *Am. J. Cardiol.* 38:170–177. https://doi.org/10.1016/0002-9149(76)90145-4

Locati, E.T., G. Bagliani, F. Cecchi, H. Johny, M. Lunati, and C. Pappone. 2019. Arrhythmias due to Inherited and Acquired Abnormalities of Ventricular Repolarization. *Card. Electrophysiol. Clin.* 11:345–362. https://doi.org/10.1016/j.ccep.2019.02.009

MacRae, C.A., and R.T. Peterson. 2015. Zebrafish as tools for drug discovery. *Nat. Rev. Drug Discov.* 14:721–731. https://doi.org/10.1038/nrd4627

McDonald, H.S., and J.E. Heath. 1971. Electrocardiographic observations on the tuatara, Sphenodon punctatus. *Comp. Biochem. Physiol. A Comp. Physiol.* 40:881–892. https://doi.org/10.1016/0300-9629(71)90277-5

Meijborg, V.M.F., B.J.D. Boukens, M.J. Janse, S. Salavatian, M.J. Dacey, K. Yoshie, T. Opthof, M.A. Swid, J.D. Hoang, P. Hanna, et al. 2020. Stellate ganglion stimulation causes spatiotemporal changes in ventricular repolarization in pig. *Heart Rhythm.* 17(5 Pt A):795–803. https://doi.org/10.1016/j.hrthm.2019.12.022

Milan, D.J., I.L. Jones, P.T. Ellinor, and C.A. MacRae. 2006. In vivo recording of adult zebrafish electrocardiogram and assessment of drug-induced QT prolongation. *Am. J. Physiol. Heart Circ. Physiol.* 291:H269–H273. https://doi.org/10.1152/ajpheart.00960.2005

Mines, G.R. 1913. On dynamic equilibrium in the heart. *J. Physiol.* 46:349–383. https://doi.org/10.1113/jphysiol.1913.sp001596

Mullen, R.K. 1967. Comparative Electrocardiography of the Squamata. *Physiol. Zool.* 40:114–126. https://doi.org/10.1086/physzool.40.2.30152446

Noble, D., and I. Cohen. 1978. The interpretation of the T wave of the electrocardiogram. *Cardiovasc. Res.* 12:13–27. https://doi.org/10.1093/cvr/12.1.13

Offerhaus, J.A., P.C. Snelderwaard, S. Algül, J.W. Faber, K. Riebel, B. Jensen, and B.J. Boukens. 2021. High heart rate associated early repolarization causes J-waves in both zebra finch and mouse. *Physiol. Rep.* 9:e14775. https://doi.org/10.14814/phy2.14775

Olson, E.N. 2006. Gene regulatory networks in the evolution and development of the heart. *Science.* 313:1922–1927. https://doi.org/10.1126/science.1132292

Pastore, J.M., S.D. Girouard, K.R. Laurita, F.G. Akar, and D.S. Rosenbaum. 1999. Mechanism linking T-wave alternans to the genesis of cardiac fibrillation. *Circulation.* 99:1385–1394. https://doi.org/10.1161/01.CIR.99.10.1385

Poelmann, R.E., and A.C. Gittenberger-de Groot. 2019. Development and evolution of the metazoan heart. *Dev. Dyn.* 248:634–656. https://doi.org/10.1002/dvdy.45

Ritchie, M.E., B. Phipson, D. Wu, Y. Hu, C.W. Law, W. Shi, and G.K. Smyth. 2015. limma powers differential expression analyses for RNA-sequencing and microarray studies. *Nucleic Acids Res.* 43:e47. https://doi.org/10.1093/nar/gkv007

Robinson, M.D., D.J. McCarthy, and G.K. Smyth. 2010. edgeR: a Bioconductor package for differential expression analysis of digital gene expression data. *Bioinformatics.* 26:139–140. https://doi.org/10.1093/bioinformatics/btp616

Schwartz, P.J., and A. Malliani. 1975. Electrical alternation of the T-wave: clinical and experimental evidence of its relationship with the sympathetic nervous system and with the long Q-T syndrome. *Am. Heart J.* 89:45–50. https://doi.org/10.1016/0002-8703(75)90008-3

Seebacher, F., and C.E. Franklin. 2001. Control of heart rate during thermoregulation in the heliothermic lizard Pogona barbata: importance of cholinergic and adrenergic mechanisms. *J. Exp. Biol.* 204:4361–4366. https://doi.org/10.1242/jeb.204.24.4361

Skeberdis, V.A., J. Jurevicius, and R. Fischmeister. 1997. Pharmacological characterization of the receptors involved in the beta-adrenoceptor-mediated stimulation of the L-type Ca2+ current in frog ventricular myocytes. *Br. J. Pharmacol.* 121:1277–1286. https://doi.org/10.1038/sj.bjp.0701268

Smirk, F.H. 1949. R waves interrupting T waves. *Br. Heart J.* 11:23–36. https://doi.org/10.1136/hrt.11.1.23

Sparks, H.V. Jr., M. Hollenberg, S. Carriere, D. Funkenstein, R.M. Zakheim, and A.C. Barger. 1970. Sympathomimetic drugs and repolarization of ventricular myocardium of the dog. *Cardiovasc. Res.* 4:363–370. https://doi.org/10.1093/cvr/4.3.363

Takeuchi, J.K., M. Ohgi, K. Koshiba-Takeuchi, H. Shiratori, I. Sakaki, K. Ogura, Y. Saijoh, and T. Ogura. 2003. Tbx5 specifies the left/right ventricles and ventricular septum position during cardiogenesis. *Development.* 130:5953–5964. https://doi.org/10.1242/dev.00797

Taylor, E.W., C.A.C. Leite, M.R. Sartori, T. Wang, A.S. Abe, and D.A. Crossley II. 2014. The phylogeny and ontogeny of autonomic control of the heart and cardiorespiratory interactions in vertebrates. *J. Exp. Biol.* 217:690–703. https://doi.org/10.1242/jeb.086199

Valentinuzzi, M.E., H.E. Hoff, and L.A. Geddes. 1969. Electrocardiogram of the snake: effect of the location of the electrodes and cardiac vectors. *J. Electrocardiol.* 2:245–252. https://doi.org/10.1016/S0022-0736(69)80084-1

Vaykshnorayte, M.A., J.E. Azarov, A.S. Tsvetkova, V.A. Vityazev, A.O. Ovechkin, and D.N. Shmakov. 2011. The contribution of ventricular apicobasal and transmural repolarization patterns to the development of the T wave body surface potentials in frogs (Rana temporaria) and pike (Esox lucius). *Comp. Biochem. Physiol. A Mol. Integr. Physiol.* 159:39–45. https://doi.org/10.1016/j.cbpa.2011.01.016

Volders, P.G.A., M. Stengl, J.M. van Opstal, U. Gerlach, R.L.H.M.G. Spätjens, J.D.M. Beekman, K.R. Sipido, and M.A. Vos. 2003. Probing the contribution of IKs to canine ventricular repolarization: key role for beta-adrenergic receptor stimulation. *Circulation.* 107:2753–2760. https://doi.org/10.1161/01.CIR.0000068344.54010.B3

Vornanen, M. 2016. The temperature dependence of electrical excitability in fish hearts. *J. Exp. Biol.* 219:1941–1952. https://doi.org/10.1242/jeb.128439

Wang, T., J. Altimiras, W. Klein, and M. Axelsson. 2003. Ventricular haemodynamics in Python molurus: separation of pulmonary and systemic pressures. *J. Exp. Biol.* 206:4241–4245. https://doi.org/10.1242/jeb.00681

Wiegerinck, R.F., A.O. Verkerk, C.N. Belterman, T.A. van Veen, A. Baartscheer, T. Opthof, R. Wilders, J.M. de Bakker, and R. Coronel. 2006. Larger cell size in rabbits with heart failure increases myocardial conduction velocity and QRS duration. *Circulation.* 113:806–813. https://doi.org/10.1161/CIRCULATIONAHA.105.565804

Yagishita, D., R.W. Chui, K. Yamakawa, P.S. Rajendran, O.A. Ajijola, K. Nakamura, E.L. So, A. Mahajan, K. Shivkumar, and M. Vaseghi. 2015. Sympathetic nerve stimulation, not circulating norepinephrine, modulates T-peak to T-end interval by increasing global dispersion of repolarization. *Circ. Arrhythm. Electrophysiol.* 8:174–185. https://doi.org/10.1161/CIRCEP.114.002195

Zaar, M., E. Larsen, and T. Wang. 2004. Hysteresis of heart rate and heat exchange of fasting and postprandial savannah monitor lizards (Varanus exanthematicus). *Comp. Biochem. Physiol. A Mol. Integr. Physiol.* 137:675–682. https://doi.org/10.1016/j.cbpb.2004.01.028

Zaar, M., J. Overgaard, H. Gesser, and T. Wang. 2007. Contractile properties of the functionally divided python heart: two sides of the same matter. *Comp. Biochem. Physiol. A Mol. Integr. Physiol.* 146:163–173. https://doi.org/10.1016/j.cbpa.2006.10.015

Supplemental material

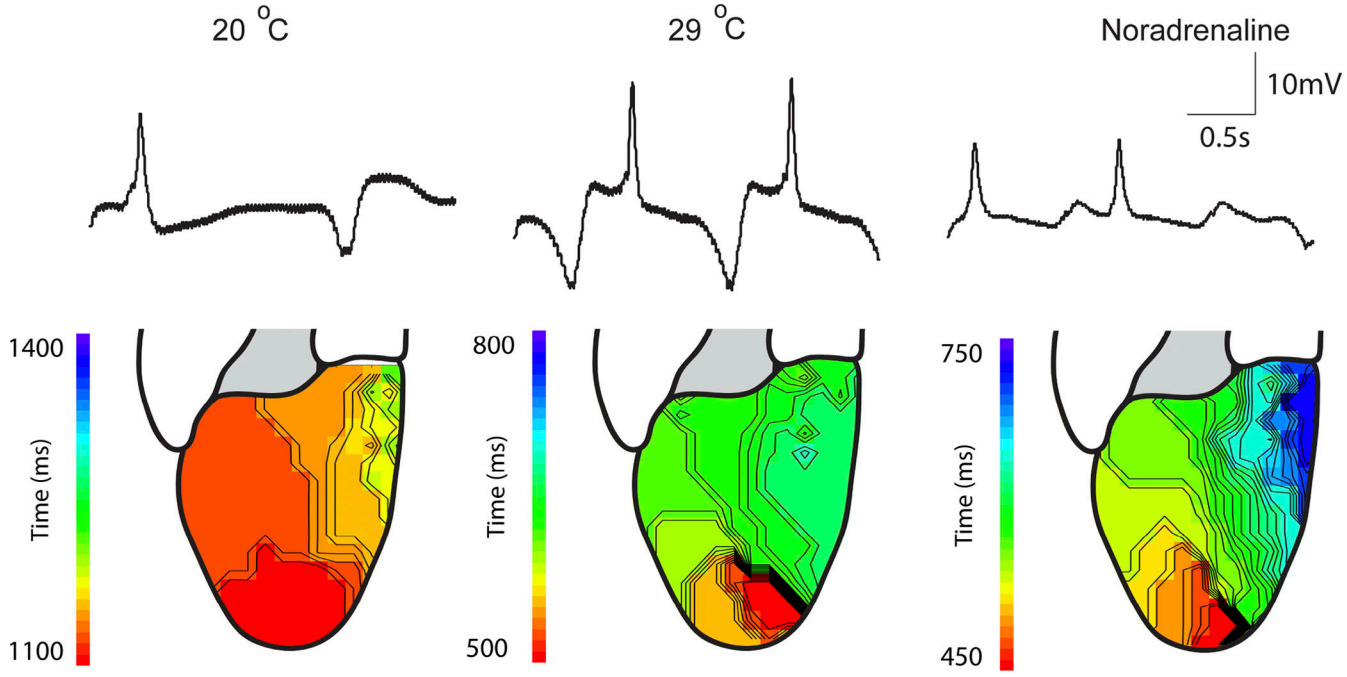

Figure S1. **Noradrenaline causes T-wave inversion.** Repolarization maps of a heart that was perfused with Ringer's solution in situ (no humoral agents) and in which the head and neck had been removed (no activity from the central nervous system). While the gradient of repolarization became steeper at higher temperatures, the administration of noradrenaline changed the repolarization vector and caused T-wave inversion (n = 1).

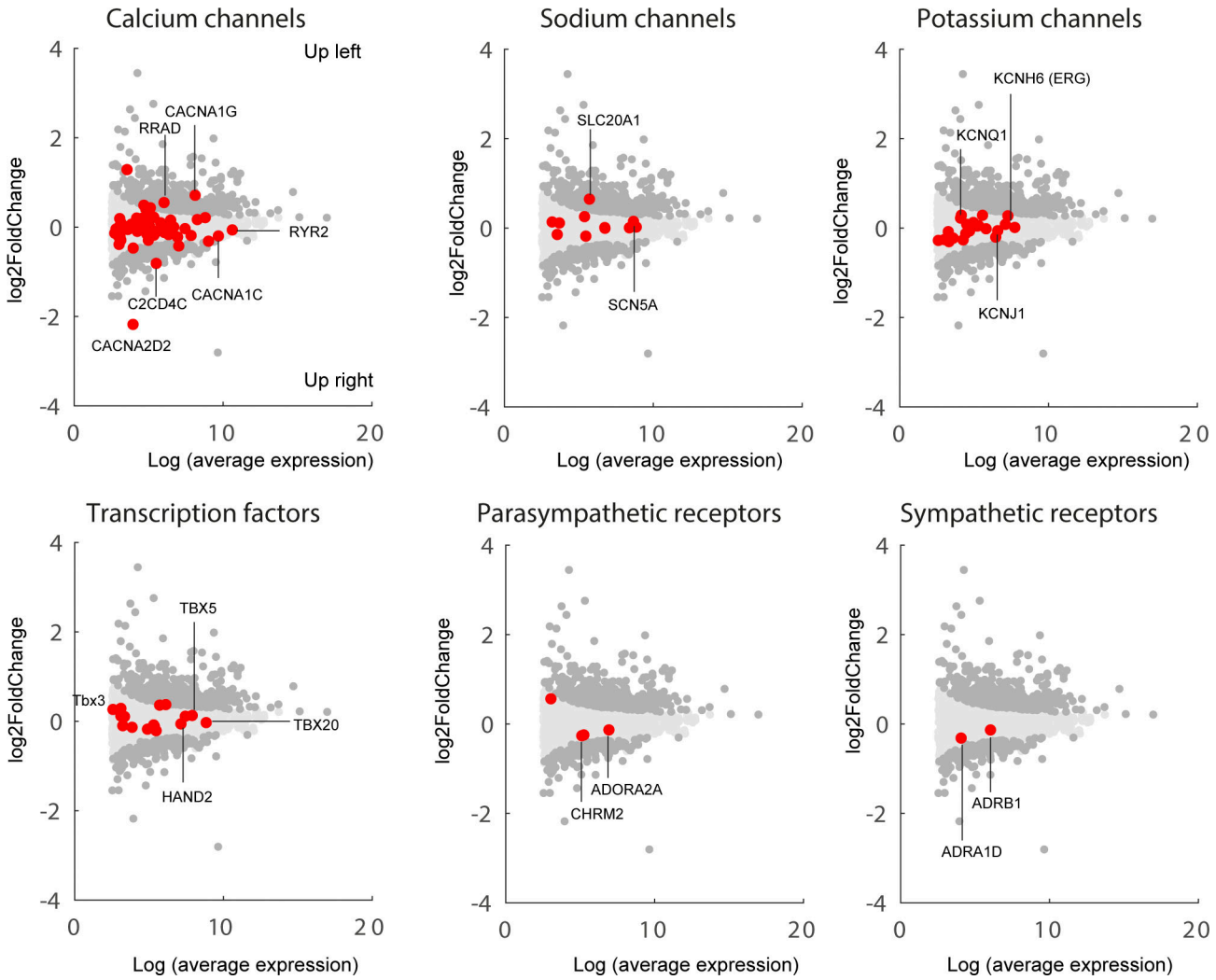

Figure S2. **Gene expression analysis of the python ventricle per category of genes.** Magnitude of expression of a gene in relation to the average expression of that gene in the four samples. The samples were collected from pythons 4 and 6 after all physiological experiments were done. P adjusted < 0.05 was considered significant (gray dots).

One table is available online as a separate file. Table S1 shows changes in ECG parameters upon heating in individual pythons measured with open chest in the presence of propranolol.